Eur. Phys. J. Spec. Top. (2022) 231:1701–1714
https://doi.org/10.1140/epjs/s11734-022-00510-z

THE EUROPEAN PHYSICAL JOURNAL SPECIAL TOPICS

Regular Article

Analytical fault impact-model for the electrical grid

Silvio Alessandroni[1,a], Maurizio Paschero[2,b], and Francesco Nicotra Menéndez[3,c]

[1] Innovation Technology Department, areti spa, Rome, Italy
[2] Grid Management System Department, areti spa, Rome, Italy
[3] Energy Transition Department, Phygital Division, Minsait, Madrid, Spain

Received 15 October 2021 / Accepted 27 February 2022 / Published online 28 March 2022

Abstract The incoming challenge of the energy transition will strongly involve the distribution system operators (DSO). The rising importance of the electricity source, the growing urban populations, and the use of alternative energies are only some of the key factors that will transform rapidly DSOs. The need to manage unpredictable flows will transform DSOs from pure distributor to dispatchers. In this context, grid resilience will become crucial to ensure the continuity of electrical service in urban areas. Shortening service restoration, thanks to technology upgrading, will improve resilience. Therefore, optimal sizing and positioning of automatic and remote-controlled switches, as well as knowledge of the effect of operational variables on the grid, will become essential for a DSO. Many studies have been conducted so far using heuristic approaches. However, the complexity of these problems grows exponentially with large grids. Consequently, numerical approaches are not suitable for operational development-planning and maintenance interventions. In this work, we derive a simple approximate analytical model which allows to make a prediction of the penalties that the DSO will pay due to user disconnections. The model relies on key constitutive and operational variables, and enables its application to optimize grid development. The model's simplicity brings the operators working on the grid closer to the problem. Moreover, its analytical nature aims to raise awareness about the relationships among the main variables responsible for the fault selection.

1 Introduction

It is expected that by 2050, around 70% of the population will live in cities. This demographic transformation will represent a big challenge for urban centers: they will need to find solutions for energy, meeting sustainability,and growth concepts. In this context, two major issues arise. First, the rapid increase of renewable energy sources introduces more unpredictability in the power grid. Second, the weight of the electricity system as critical infrastructure for development, safety, and quality of life in industrialized countries is growing.

Over the years, critical infrastructures have become increasingly complex and interdependent, and the malfunction of one of these can cause real inconveniences. Interdependencies between critical infrastructures have been modelled. Several stress tests, using simulation tools, have demonstrated the essential role that electrical grids play in the functionality of other public services [1]. Indeed, any failure in the electrical service could lead to the interruption of activities in the industrial, domestic, and health worlds [2,3]. Preventive maintenance and the ability to react promptly when a breakdown is detected are extremely important.

In addition, service interruptions can lead to production losses, restart costs, equipment damage, and customer dissatisfaction [4]. Distribution system resilience, defined in [5] as "the ability to withstand and reduce the magnitude and/or duration of disruptive events, which includes the capability to anticipate, absorb, adapt to, and/or rapidly recover from such an event", is, therefore, essential for both citizens and utilities.

To incentive utilities to improve their distribution service, regulators adopt Performance-Based Schemes (PBS) [6]. They rely on grid's performance benchmarks which measure the average user interruption. The most common indicators are: System Average Interruption Index (SAIDI), System Average Interruption Frequency Index (SAIFI), and Momentary Average Interruption Frequency Index (MAIFI) [6]. PBSs reward or penalize utilities for good or poor resilience, which inevitably becomes crucial for utilities.

In a typical radial distribution system, a failure of any component will cause an interruption for all loads downstream and upstream of the faulty zone, until the faulty portion is identified and isolated to allow service restoration. Hence, fault detection, location, and isolation are pivotal building phases to shorten restoration time after an outage and reduce the number of users

[a] e-mail: silvio.alessandroni@areti.it
[b] e-mail: maurizio.paschero@aceaspa.it (corresponding author)
[c] e-mail: fnicotra@minsait.com

impacted by the fault [4]. Consequently, improving the efficiency of these phases boosts resilience indexes. A first approach to improve resilience is by developing methodologies to accelerate the fault location phase [7]. Though this approach surely improves resilience, it has a limited impact on the isolation procedure, which mainly relies on grid switching technology. This is where remote-controlled and automated secondary substations (SS) play a crucial role. Indeed, these are recognized as one of the most effective technological solutions adopted by utilities to significantly improve service restoration, as they can speed up or automate both fault detection and isolation. The main issues for the application of this solution rely on the determination of the number, location, and type of remote-controlled and automated devices to be installed throughout the grid's SSs. It results in a combinatorial constrained optimization problem [8], whose complexity grows exponentially with the number of SSs on the grid.

Due to the nature of the problem, most of the existing publications propose a mixed integer linear programming (MILP) approach [7–10]. Although miscellaneous objective functions have been constructed to address the problem, almost all those works propose meta-heuristic approaches. These solutions may not be adequate when dealing with large grids. In this context, we believe that the analytical approach proposed in this paper and meta-heuristic methods complement themselves synergistically. Indeed, this method allows to easily compute approximate optimal solutions that can be used to narrow the search space of the most accurate numerical models. Moreover, the approximate analytical model can be used by a DSO to quickly carry out useful preliminary planning.

Literature on this topic can be broadly cataloged with respect to the cost function used in the optimal automation devices allocation problem.

An overview of the main previously mentioned miscellaneous cost functions suggested by literature to model the optimal automation devices allocation problem is proposed. In [9–11], the cost to users due to long-term interruptions is taken into consideration. In [12, 13], the cost due to short-term interruptions is added to the cost function. The papers [14,15] directly consider resilience indexes optimization (MAIFI, SAIFI, and SAIDI) explicitly. The cost of new automation devices is considered in [13] and [16]. In [10], the relocation cost of the existing automated SSs is also considered. Moreover, in [10], the cost of Distributed Generators, load curtailment possibility, and operational constraints (voltage and thermal) are also contemplated in the cost function. Another cost function criteria used to determine the optimal composition and placement of automated SSs are loss minimization and load equalization [9]. In [17], the authors pursue the minimization of total expected energy not served. Most of these approaches do not deal with the uncertainty of many operational factors that impact grid's reliability [18], for this reason in [16] the uncertainties in loads, failure rates, and interruption duration have been considered (triangular fuzzy numbers). In [12], authors pursue allocation optimization adding the cost of maintenance to the model. In [19], researchers develop a model with the objective of minimizing the investment, operation, maintenance, and unreliability costs. Along with this last approach, various asset management strategies in the distribution grids based on short-term, mid-term, and long-term time scales are proposed in [20]. A multi-objective decision-making condition-based maintenance model is proposed in [21]. The theory of life cycle asset management within the cutting-edge technology in smart grid is analyzed in [22].

Another distinction among existing studies entails the specific heuristic algorithms used in the implementation. In [23], the proposed mathematical problem based on a multi-objective formula is solved with a genetic algorithm. In [24], a commercial simulator is used after the formulation as a mixed integer convex programming problem. In [16], a fuzzy mixed integer linear programming algorithm is applied. In [11], the costs of allocation and energy not supplied are minimized using a memetic algorithm with a structured population. In [25], authors solve the problem with multi-objective particle swarm optimization algorithm. In [26], a method to reach a sub-optimal solution applying an algorithm that works in polynomial time and relies on a logarithmic approximation ratio of the maximum number of load zones in a feeder is proposed. In [27], an immune algorithm optimal allocation that chases the minimization total cost of user disservice and cost of automation devices is used. In [28], a simulation tool, able to assess electrical grid resilience, is recognized to be particularly suited to provide sub-optimal automation positioning, selected using heuristic strategies.

Due to their complexity, DSOs are not used to applying numerical models for macro-planning to orient their budget. Indeed, simpler cost–benefit evaluation methods are adopted. The numerical models are mostly used to address and optimize specific interventions once the macro-plannings have been assigned.

We strongly believe that the analytical approximated approach, which is proposed in this work to model the fault restoration process, gives a new useful supplemental tool for the DSO to better plan its interventions. Indeed, it represents an optimal compromise between the forecast precision, which can be given by a complex numerical model and the operating simplicity proper of a simple cost–benefit analysis mostly based on flat average values. The proposed analytical model can be thus used by a DSO to better orient its budget when dealing with strategic scenarios of long period investment planning. At the same time, it can be used to narrow the search space of the most accurate numerical models which are used to program specific interventions on the grid.

The paper is organized as follows. First, we present an overview of the medium-voltage service restoration process (in Sect. 2). Then, we calculate the complexity of the allocation optimization problem for heuristic approaches (in Sect. 3). Finally, we present the analytical failure impact-model derivation (in Sect. 4) and its

operative application is discussed and compared to real data (in Sect. 5). Concluding remarks are in Sect. 6.

2 Electrical distribution grids' background

Most of Medium-Voltage (MV) distribution grids present structural loops even if they are usually exerted radially (Fig. 1). The meshed structure implies that each SS, also referred in the following as node, can be fed at least by two alternative ways generally powered from two different Primary Substations (PS) (see Fig. 1). Radial operation implies that only one of the possible supply paths can be active during operation. Meanwhile, the other supply route (guaranteed by feeders alternative to the main one, also called counterfeited feeder) works as a back-up in case of failure on the main feeder. The counterfeited feeder can be activated through the closure of an appropriate switch installed on the edge SS, which determines the endpoint between a feeder and its counterfeited feeder (see Fig. 1).

The MV feeder topology is determined by the status of the switches in each node. Each SS is generally equipped with at least three MV switches. Two switches interconnect the actual node with the SS sited upstream (in switch) and downstream (out switch). The third one interconnects the MV busbar to the MV/LV transformer feeding the Low-Voltage (LV) user underlying the SS.

There exist three different kinds of switches: manual switches, which require the intervention on field of a human operator in the SS to be operated; remote-controlled switches, which can be maneuvered remotely by an operator through a suitable telecommunication network; and automated switches, which do not require any human intervention to operate.

When both the in and out switches of a given SS are closed, the actual node is fed by the upstream SS and it feeds all the downstream nodes of the feeder until the edge SS (represented in Fig. 1) which has its out switch open. When a feeder's branch failure occurs (see Fig. 2), the appropriate opening of the switches present in the upstream and downstream SS allows the sectioning of the faulty part of the feeder; while the reclosure of the out switch on the edge SS allows the repowering of the portion of the feeder downstream of the fault.

The fault-selection process is divided into three sequential phases: field automatic selection (0–1 s), remote-control selection (1–15 min), and field manual selection by Work Force Management (30–90 min).

Automatic phase can be performed by a unilateral or a bilateral approach. When dealing with the unilateral

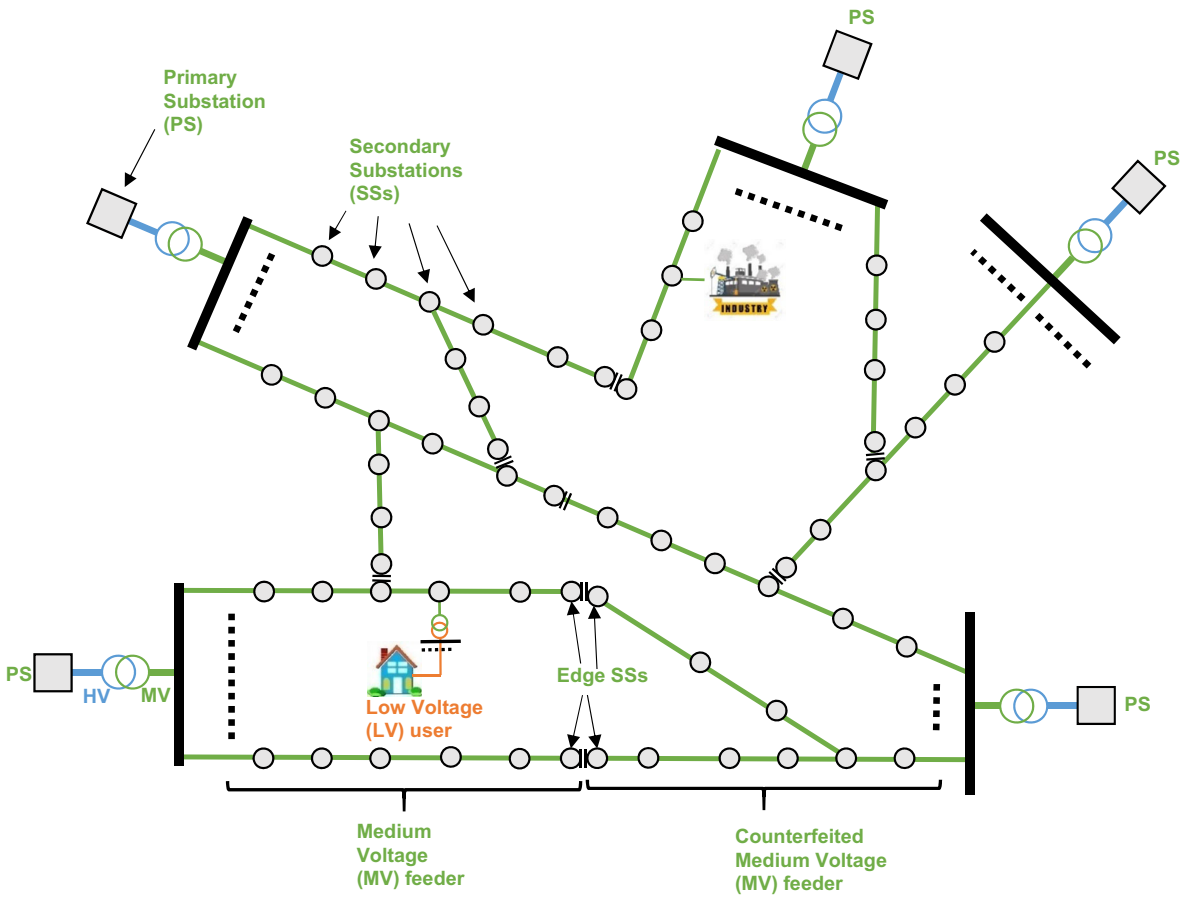

Fig. 1 Medium voltage distribution grid scheme

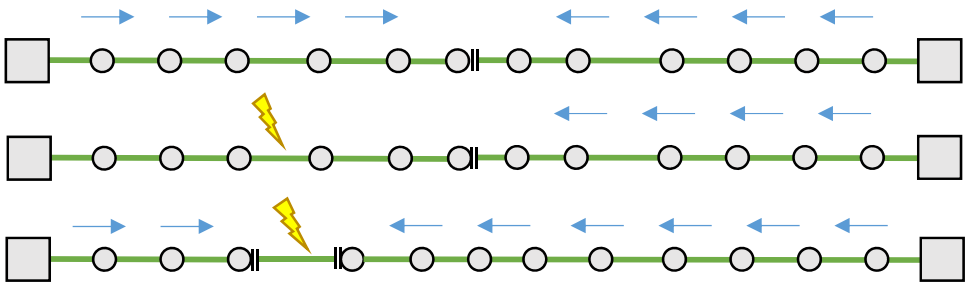

Fig. 2 Fault isolation procedure by repowering from the counterfeited feeder

solution, a fault event on a feeder brunch determines the tripping of the first switch upstream of the fault (if there are no automatic switches present in the SSs upstream of the fault, the switches in the PS will automatically open). This automation is carried out on a purely chronometric basis and does not need to establish any communication among the automated SS, and it is able to select only the faults that occur downstream of a switch (by preserving the upstream portion of the feeder to its disconnection). The repowering of the portion downstream of the fault is not operated automatically and needs to go through further phases. Otherwise, when dealing with a Bilateral solution, the switches along the feeder are enabled to communicate with each other, so that the automatic procedure is able to repower both the portions of the feeder upstream and downstream of the automatic switches that select the fault. Once the automatic phase is concluded, the remaining fault isolation is conducted with a trial and error procedure aimed to repower half of the still unpowered portion of the feeder at each step. This procedure is usually referred to as dichotomous procedure.

Remote-controlled phase is performed by opening one of the switches of one of the nodes which divides into two portions the unsupplied segment. Remotely, an attempt to reset the tripped switch to repower the first portion of the segment is done. If this first portion remains supplied without a new trip of the switch upstream of the feeder, it means that the fault is downstream of the node on which the operator has intervened remotely. Otherwise, if the switch trips again, it means that the fault is on the upstream portion of the node on which the operator has implemented the interruption. This dichotomous search algorithm: disconnect in the middle and look for the fault between the two unsupplied portions (dichotomies) will continue until the remotely controllable SSs are exhausted.

Manual phase finally operates the final reduction of the faulty portion with complete repowering of the users. It takes place by manually operating the switches in the field by means of teams of operators sent to the SSs. Also, in this case, a dichotomous procedure is operated with the only difference that the manual handling and the movement between the SSs will require much more time than the reduction in remote control.

3 Computational complexity analysis

To motivate the development of an analytical model, a brief derivation of the computational complexity of a brute force approach is presented herein. A brute force approach (also called exhaustive search) consists in calculating the results of all possible candidates for a problem solution, checking their values, and choosing the optimal one.

The optimal allocation problem depends on the determination of the number and location of remote and automatic switches among the nodes. Each transformation of a manual node into a remote-controlled or automated one results in a different fault risk reduction. The objective of the problem is to maximize the benefit obtained with those transformations in terms of grid's fault reduction. The risk of a branch fault can be defined as the product between the branch fault rate and the fault's impact. The fault impact depends on the distribution of the users subtended to the nodes involved by the fault and the service restoring procedures.

The above-mentioned brute force approach applied to this case would consist in determining all the benefits of transforming the manual switches into automation/remote-controlled ones, for all the nodes in a feeder (with a given budget and operational constraints). Then, the optimization procedure needs to be repeated feeder by feeder.

By defining N_M, N_R and N_A as the total amount of electric SSs in an electric feeder that allow manual, remote-controlled, and automatic maneuvering, respectively, an assigned set of the three variables $N_{A_i}, N_{R_i}, N_{M_i}$ will be referred as the ith fundamental set-up of a given feeder.

By defining $N_{\mathrm{TOT}} = N_M + N_R + N_A$, the total amount of SSs in the feeder, the number of fundamental set-up for a feeder N_{FS} can be calculated as

$$N_{\mathrm{FS}} = \frac{(N_{\mathrm{TOT}} + 2)\,(N_{\mathrm{TOT}} + 1)}{2}. \tag{1}$$

Equation (1) can be easily understood considering the Gauss sum of the first $N_{\mathrm{TOT}} + 1$ fundamental set-ups. In Fig. 3 part (a), all the fundamental set-ups of a feeder having 4 SSs are shown in the (N_R, N_A) plane. The total number of set-ups can be obtained by adding $N_{\mathrm{TOT}} + 1$ rows having a length ranging from 1 to $N_{\mathrm{TOT}} + 1$.

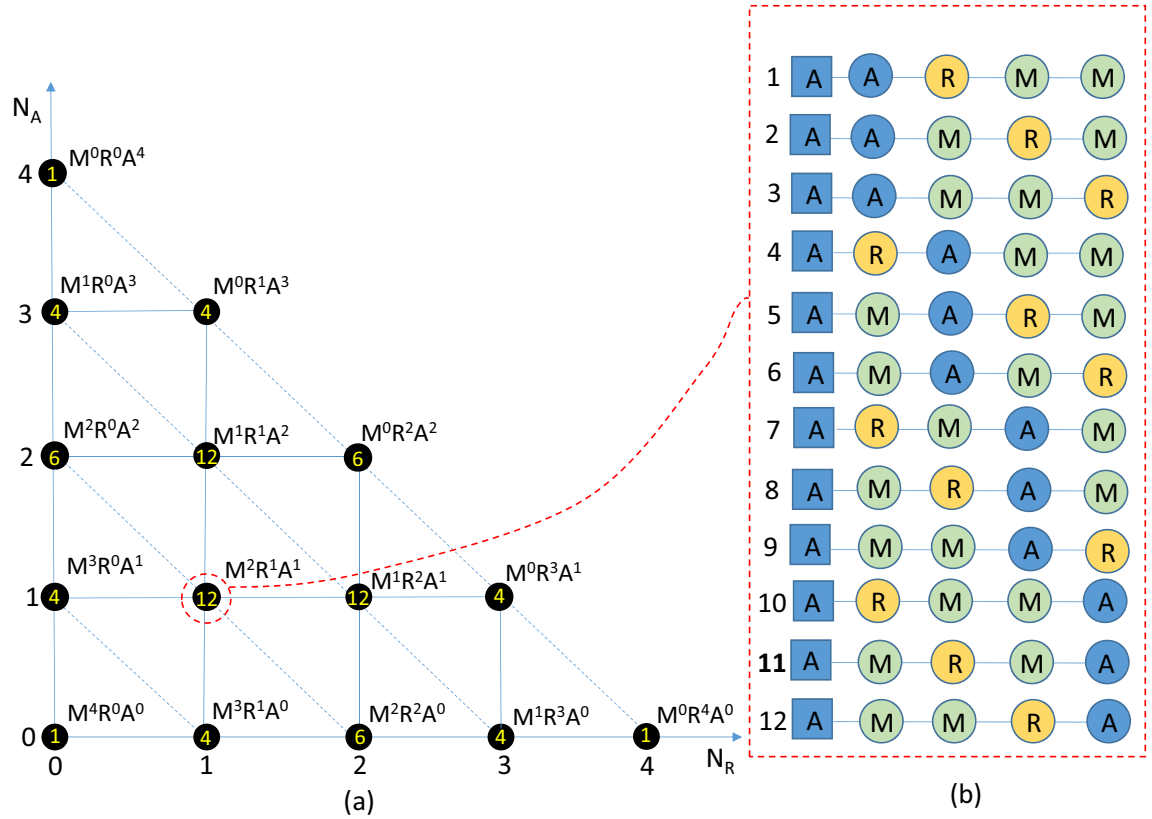

Fig. 3 Example of fundamental set-up: **a** representation for $N_{\mathrm{TOT}} = 4 \rightarrow N_{\mathrm{FS}} = 15$; **b** enumeration of all the 12 configurations of the fundamental set-up $\mathrm{M^2R^1A^1}$

The ith N_{FS} fundamental set-ups will be described with the following notation: $M^{N_{M_i}} R^{N_{R_i}} A^{N_{A_i}}$. For example, a feeder with 6 nodes of which 2 are remote-controlled and 1 is automated will be described as $M^3 R^2 A^1$.

For the ith fundamental set-up, the $N_{A_i} + N_{R_i} + N_{M_i} = N_{\mathrm{TOT}}$ SSs can be distributed along the feeder in different orders. Each possible order will be referred as a configuration. The number of possible configurations n_i^{cnf} for the ith fundamental set-up is a permutation with repetitions and can be calculated using the multinomial coefficient

$$n_i^{\mathrm{cnf}} = \binom{N_{\mathrm{TOT}}}{N_{A_i}, N_{R_i}, N_{M_i}} = \frac{N_{\mathrm{TOT}}!}{N_{A_i}! N_{R_i}! N_{M_i}!}. \quad (2)$$

Finally, using the multinomial theorem, it can be shown that the total number of possible configurations in a feeder having N_{TOT} SS is

$$\sum_{i=1}^{N_{\mathrm{FS}}} n_i^{\mathrm{cnf}} = \sum_{i=1}^{N_{\mathrm{FS}}} \binom{N_{\mathrm{TOT}}}{N_{A_i}, N_{R_i}, N_{M_i}} = 3^{N_{\mathrm{TOT}}}. \quad (3)$$

The complexity of the whole grid can be calculated by adding the complexity of each feeder given by (3) for all the feeders in the grid.

As an example, the 15 fundamental set-ups obtained for $N_{\mathrm{TOT}} = 4$ are represented as the black dots in Fig. 3 part (a).

For each dot is shown in yellow text the number of configurations associated with the corresponding fundamental set-up calculated according with (2). It is easy to verify that the sum of the 15 values written in the black dots yields the value $81 = 3^4$ as stated by (3). As an example in part (b) of Fig. 3 are enumerated the 4!/(2!1!1!)=12 configurations associated with the fundamental set-up $\mathrm{M^2R^1A^1}$.

It is interesting to note that, apart from the eleventh one, none of the 12 configurations enumerated in Fig. 3 part (b) has particular symmetries. The symmetry of the eleventh configuration makes it particularly efficient. Indeed, the number of operations necessary to select a fault for this symmetrical configuration is independent of the branch on which the fault occurs. It can be understood that this is equivalent to saying that this symmetry minimizes the average number of manouvres necessary to select a fault on any branch of the feeder.

In Sect. 4, it will be shown how this special symmetry can be used to derive a useful analytical model.

Given a fundamental set-up for each configuration, it is necessary to calculate the total risk given by the sum of all feeder's branch risks and choose the configuration with the lowest risk. The risk associated with a single component is calculated by multiplying the impact related to the failure of the component in terms

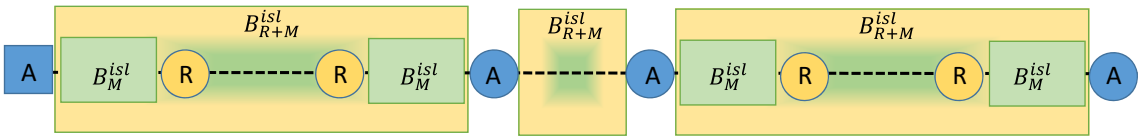

Fig. 4 Graphical representation of the model assumptions. Automatic, remote-controlled, and manual SSs are represented in blue, yellow, and green, respectively

of total minutes of disconnection suffered by the users (and/or in terms of disconnected users) by the failure rate of the component itself. For each of the fundamental set-ups, there is one configuration that minimizes the associated risk. By choosing the minimum value among the risks underlying the optimal configuration for each fundamental set-up, it is possible to design the optimal automation conjunction in terms of underlying risk reduction. Based on the previous discussion, it is possible to understand that this configuration capable of minimizing the risk is connected to the symmetry of the feeder as mentioned in the previous part of this section.

Once the previous risk calculation has been addressed, it is simple to build the optimal sizing and location problem by simply introducing the installation and maintenance cost of automatic and remote-controlled switches that reduce the risk of a given feeder.

In accordance with previous arguments, the computational complexity of the brute force approach to the stated problem solution increases exponentially with growing dimension of the grid. It is therefore useful to adopt complexity reduction strategies.

In this work, an analytical model, capable of exploiting the positive characteristics of the symmetries of the feeders, is developed.

4 Derivation of the proposed model

4.1 General definitions

To introduce the failure's impact-analytical calculation model, all the assumptions needed to derive the model are first stated. In this work, it is assumed that all the constitutive variables are uniformly distributed along the feeder. More precisely, it is supposed that each SS of the feeder has the same amount of users U_{SS}, the N_A automated SSs are uniformly distributed along the feeder and the N_R remote-controlled and the N_M manual SSs are dichotomously distributed between two adjacent automated SSs. The previous assumptions allow simplifying the peculiar topological structure of each feeder. These hypotheses take for granted that all portions of a feeder with a given number of nodes have the same behavior in terms of fault isolation. It is also assumed that each branch has the same failure rate. Although these assumptions seem restrictive, it should be noted that a well-designed feeder must tend to a uniform distribution of all the presented quantities along the feeder. In this way, a modelled feeder tends to represent the ideal case. The previously presented assumptions are resumed in Fig. 4.

Obviously, these assumptions are necessary to derive an analytic closed form of the model and introduce consistent approximations of reality. However, most of those are also DSO's drivers used to design and operate on the feeders. To have a first measure of the impact introduced by these approximations, paragraph 5.2 shows a comparison between the fault impact predicted by the model and the real impact cumulated in a set of real fault occurred in 2020 on *a*reti grid.

According to Fig. 4, the number of branches B^{isl}_{R+M} that belong to the automation island (i.e., the portion of the feeder to be repowered after the end of the automatic selection phase using remote and manual maneuvers—see yellow/green boxes in Fig. 4) is

$$B^{\mathrm{isl}}_{R+M} = \frac{N_{\mathrm{TOT}}}{N_A}. \tag{4}$$

Assuming that all the automated SSs have automatic switches in both the input and output side of the feeder, the users of each automated SS will be always automatically repowered and the number of SSs N^{isl}_{R+M} that belongs to the remote and manual island (see yellow/green boxes in Fig. 4) is

$$N^{\mathrm{isl}}_{R+M} = B^{\mathrm{isl}}_{R+M} - 1. \tag{5}$$

Similarly, considering that an automated SS can be also remote-controlled, the number of branches B^{isl}_{M} that belongs to the manual island (i.e., the set of branches to be repowered in the manual selection phase—see green rectangle in Fig. 4) is

$$B^{\mathrm{isl}}_{M} = \frac{N_{\mathrm{TOT}}}{N_R + N_A}. \tag{6}$$

Assuming that all the remote-controlled SSs have remote-controlled switches in both the input and output sides of the feeder, the users of each remote-controlled SS will be always repowered during the remote-control phase, implying that the number of SSs N^{isl}_{M} that belong to the manual is

$$N^{\mathrm{isl}}_{M} = B^{\mathrm{isl}}_{M} - 1. \tag{7}$$

If all the manual SSs have manual switches in both the input and output sides of the feeder, the users of each manual SS will be always repowered during the manual phase, implying the complete selection at the fault.

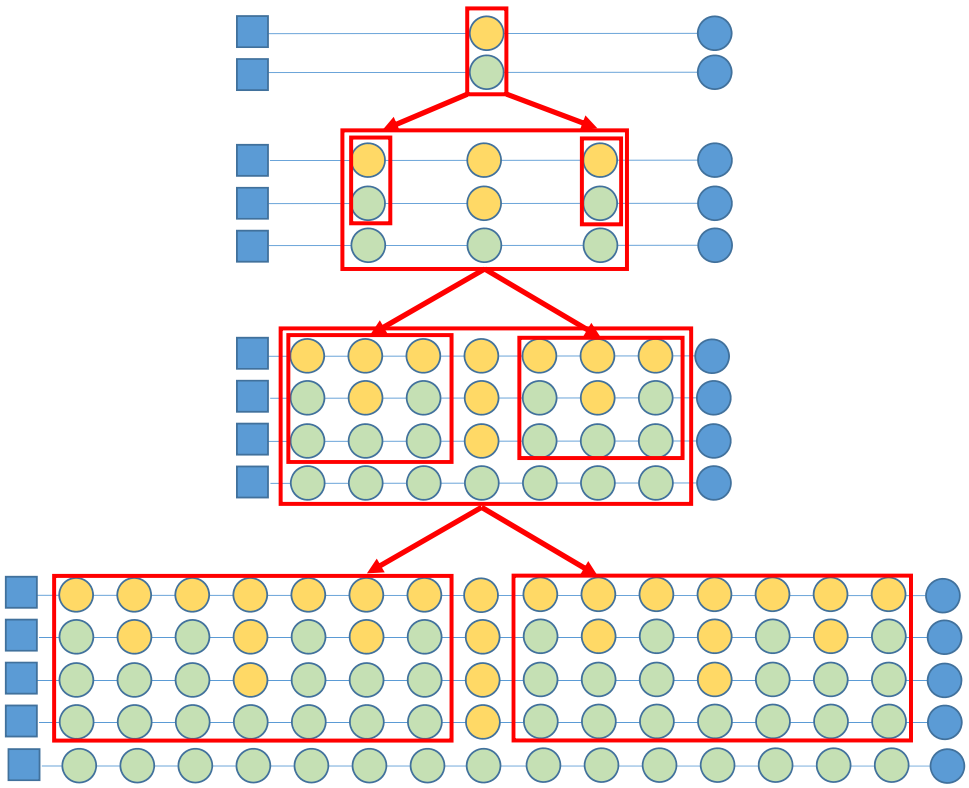

Fig. 5 Dichotomous structure scaling with incremental complexity

The derivation for an ideal bilateral automated feeder fault-selection is first presented. Then, the unilateral automated feeder case is derived by adding an extra term to the bilateral case. Finally, the non-ideal cases that consider the non-dichotomous structure of a feeder and the non-ideal effectiveness of the automatic and remote-control technologies are briefly discussed and will be extended in future works.

In the proposed model, the edge SS of each given feeder is assumed to be automated (i.e., N_A>=1). This requirement is needed to keep the symmetry of the feeder given by the presence of the PS automatic breaker, which fed the first SS. It should be noted that N_A =1 implies that in case of bilateral automation the automatic SS will just repower its own users (by commutating both its automatic upstream and downstream switches); while in the case of unilateral automation the last SS, cannot operate automatically, and it will work as a remote-controlled one.

To evaluate the number of steps needed to repower the whole feeder, we assume, after the end of the automatic phase, the use of a dichotomous fault-selection procedure that at each step halves the number of disconnected branches in a hierarchical way using remote-control and manual maneuvers. The application of the dichotomous procedure requires the feeder to have a special structure that can be derived using the recursive procedure described in Fig. 5.

According to the dichotomous structure shown in Fig. 5, the number of steps s_{R+M} needed to repower the entire feeder using remote-controlled and manual maneuvers is equal to

$$s_{R+M} = \log_2(B^{\text{isl}}_{R+M}) \rightarrow B^{\text{isl}}_{R+M} = 2^{s_{R+M}}. \tag{8}$$

Similarly, the number of manual steps needed to repower the manual island after the remote-control phase depends on the number of branches B^{isl}_M as

$$s_M = \log_2\left(B^{\text{isl}}_M\right) \rightarrow B^{\text{isl}}_M = 2^{s_M}. \tag{9}$$

The number of remote-controlled steps can be calculated as

$$s_R = s_{R+M} - s_M. \tag{10}$$

Using (8) and (9), the following relation can be found:

$$\frac{B^{\text{isl}}_{R+M}}{B^{\text{isl}}_M} = \frac{2^{s_{R+M}}}{2^{s_M}} \quad = \quad 2^{s_R} \rightarrow B^{\text{isl}}_{R+M} = 2^{s_R} B^{\text{isl}}_M. \tag{11}$$

It is important to remark that the duration of each step must be understood in the medium sense, since during the application of the dichotomous procedure, it may happen that a circuit breaker is closed on failure. In this case, it is necessary to retrace one's steps and isolate the other half of the feeder, effectively lengthening the halving of the disconnected section.

The number of SSs N^{out}_i disconnected during the *ith* step of the dichotomous procedure is

$$N^{\text{out}}_i = \frac{B^{\text{isl}}_{R+M}}{2^{i-1}} - 1 \ \text{ for } i = 1, \ldots, s_{R+M}. \tag{12}$$

It is possible to derive S^{out}_{R+M} as the cumulated number of the SS interruptions needed to completely repower the entire automated island by means of the dichotomous procedure during the remote and manual selection phase

$$S^{\text{out}}_{R+M} = \sum_{i=1}^{s_{R+M}} N^{\text{out}}_i = \sum_{i=1}^{s_{R+M}} \left(\frac{B^{\text{isl}}_{R+M}}{2^{i-1}} - 1 \right) = \sum_{j=0}^{s_{R+M}-1} \left(\frac{B^{\text{isl}}_{R+M}}{2^{j}} - 1 \right). \tag{13}$$

Considering (10) and the geometric series summation, (13) becomes

$$S^{\text{out}}_{R+M} = 2B^{\text{isl}}_{R+M} \left(1 - \frac{1}{2^{s_{R+M}}} \right) - s_{R+M} = 2\left(2^{s_R}2^{s_M} - 1\right) - s_R - s_M. \tag{14}$$

Similarly, it is possible to derive S^{out}_{M} as the cumulated number of the SS interruptions needed to completely repower the manual island during the manual selection phase

$$S^{\text{out}}_{M} = \sum_{i=s_R+1}^{s_{R+M}} N^{\text{out}}_i = \sum_{j=0}^{s_M-1} \left(\frac{B^{\text{isl}}_{R+M}}{2^{j}2^{s_R}} - 1 \right) = \sum_{j=0}^{s_M-1} \left(\frac{B^{\text{isl}}_{M}}{2^{j}} - 1 \right) = 2\left(2^{s_M} - 1\right) - s_M. \tag{15}$$

4.2 Ideal case impact model

Using the previous definitions, it is now possible to derive the model of the three impact Key Performance Indicators (KPI) T, U and D describing the total time needed to complete the service restoration, the total number of disconnected users during the fault, and the cumulated duration of all users disconnection. U KPI is the base for the calculation of SAIFI index, whereas the D KPI is the base for the calculation of SAIDI index.

An analytical derivation of the three KPIs for both the bilateral and the unilateral case is described in the following. As shown in Fig. 6 when a fault occurs in the *ith* automation island of a feeder having the bilateral automation the automatic switches suddenly commutate to select the nodes sited between the closer automatic SSs located upstream and downstream the fault respectively.

In this case, the T_{Bil} impact defined in terms of total time spent to completely restore the users of the feeder depends on the set-up times t_{0R} and t_{0M} and the specific inter-maneuvering time t_R and t_M associated with the remote-controlled and manual phases, respectively, as

$$T_{\text{Bil}} = (t_{0R} + t_R s_R) + (t_{0M} + t_M s_M). \tag{16}$$

Similarly, the U_{Bil} impact defined in terms of the total number of users disconnected by the fault can be obtained as

$$U_{\text{Bil}} = U_{\text{SS}} N^{\text{isl}}_{R+M} = U_{\text{SS}}(2^{s_R}2^{s_M} - 1). \tag{17}$$

The D_{Bil} impact defined in terms of the sum of all user interruption durations can be now derived by adding the corresponding set-up and inter-maneuvering impacts for both remote-controlled and manual phases. The calculation of set-up impact is elementary, while for the inter-maneuvering impact, we can consider the sum of the SSs interruption calculated (13) and (15) applied to both the remote-controlled and manual phases each one multiplied by its own inter-maneuvering time

$$\begin{aligned} D_{\text{Bil}} &= U_{\text{SS}} \left(t_{0R} N^{\text{isl}}_{R+M} + t_R \left(S^{\text{out}}_{R+M} - S^{\text{out}}_{M} \right) \right. \\ &\quad \left. + t_{0M} N^{\text{isl}}_{M} + t_M S^{\text{out}}_{M} \right) \\ &= U_{\text{SS}} \left(t_{0R} \left(2^{s_R}2^{s_M} - 1\right) + t_{0M} \left(2^{s_M} - 1\right) \right. \\ &\quad + t_R \left(2\left(2^{s_R} - 1\right)2^{s_M} - s_R \right) \\ &\quad \left. + t_M \left(2\left(2^{s_M} - 1\right) - s_M \right) \right). \end{aligned} \tag{18}$$

As shown in Fig. 7, the unilateral automation instantly reduces the fault, so that the interruption is limited to the branches downstream the first automated SS that is found upstream the fault.

This means that the fault will be in the automation island located between the automated SS, which reacts to the fault, and the next one.

Oppositely to the bilateral scenario, in the unilateral case, the remote-control room should isolate the island

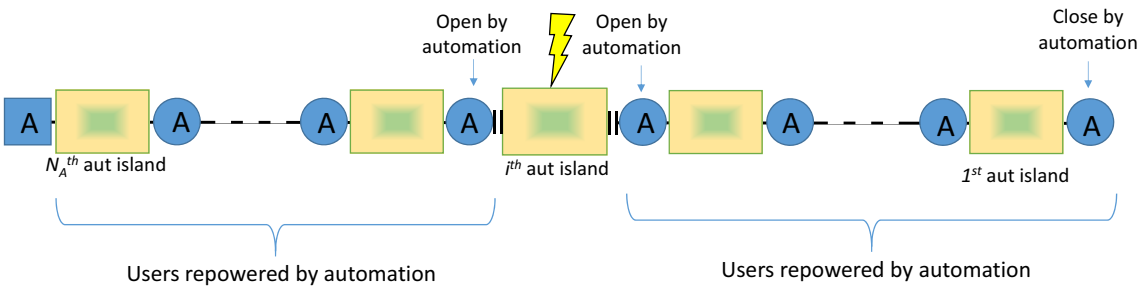

Fig. 6 Fault isolation in a bilateral automation scenario

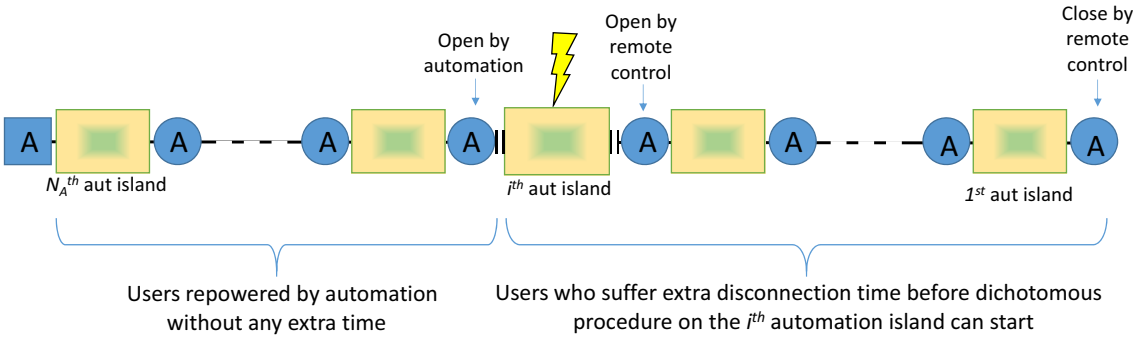

Fig. 7 Fault isolation in a unilateral automation scenario

affected by the fault, by repowering all the users downstream of the automation island affected by the fault before the dichotomous procedure can start.

According to the previous arguments, the T_{Uni} impact of the unilateral configuration can be calculated by adding to the T_{Bil} impact the inter-maneuvering time t_R needed to operate remotely the counterfeited SS, as shown in Fig. 7

$$T_{\mathrm{Uni}} = T_{\mathrm{Bil}} + t_R. \tag{19}$$

The number of users involved in the extra remote-control step when a fault happens on the *ith* automation island is

$$U_i^{\mathrm{ext}} = U_{\mathrm{SS}} \left(i \left(N_{R+M}^{\mathrm{isl}} + 1 \right) \right) = U_{\mathrm{SS}} i B_{R+M}^{\mathrm{isl}}. \tag{20}$$

In this case, the fault impact in terms of the number of SSs involved in the extra remote-controlled step depends on the location of the automation island where the fault occurs. Indeed, when the fault occurs on the *ith* automation island, there will be i automated islands and i automated SSs involved in the extra remote-controlled step (see Fig. 7).

This consideration leads to assuming the U impact of the unilateral automation as the average of the registered impact of all the possible fault scenarios (this can be done, because it has been assumed a uniform fault rate among the different fault scenarios).

The U_{Uni} KPI for the unilateral automation is

$$\begin{aligned} U_{\mathrm{Uni}} &= \frac{1}{N_A} \sum_{i=1}^{N_A} U_i^{\mathrm{ext}} = \frac{1}{N_A} \sum_{i=1}^{N_A} U_{\mathrm{SS}} i B_{R+M}^{\mathrm{isl}} \\ &= U_{\mathrm{SS}} \frac{B_{R+M}^{\mathrm{isl}}}{N_A} \sum_{i=1}^{N_A} i \\ &= U_{\mathrm{SS}} \frac{B_{R+M}^{\mathrm{isl}}}{N_A} \frac{(N_A+1)\, N_A}{2} \\ &= U_{\mathrm{SS}} 2^{S_{R+M}} \frac{(N_A+1)}{2} = (U_{\mathrm{Bil}} + U_{\mathrm{SS}}) \\ &\quad \frac{(N_A+1)}{2}. \end{aligned} \tag{21}$$

The latter term of (21) shows that the unilateral automation behaves mostly as the bilateral one when $N_A = 1$ (i.e., when the edge SS is the only automated SS in the feeder). The additional term U_{SS} represents the users of the edge SS who must be remotely repowered from the operating control room.

To derive the D impact for the unilateral scenario, it should be understood that all the users involved in the extra remote-control step suffer an additional inter-maneuvering time t_R before the feeder is brought back to the conditions of the bilateral automation scenario. Consequently, the unilateral D KPI can be obtained by adding the bilateral one with an extra term

$$\begin{aligned} D_{\mathrm{Uni}} &= D_{\mathrm{Bil}} + U_{\mathrm{Uni}} t_R \\ &= D_{\mathrm{Bil}} + U_{\mathrm{SS}} 2^{s_R} 2^{s_M} \frac{(N_A+1)}{2} t_R. \end{aligned} \tag{22}$$

4.3 Non-ideal case discussion

The exact dichotomous structure, assumed in this paper for simplicity of derivation, is infrequent in real grids, although they are usually designed to approximate the ideal structure (it can be intuitively understood that it is the best choice to optimize the partitioning of the fault-selection problem).

It can be understood that each pair (s_R, s_M) is biunivocally related to a dichotomic feeder, as shown in Fig. 8, where the case $N_{\mathrm{TOT}} = 8$ is depicted.

Indeed, it can be realized that a fault on a branch of a generic feeder having the same number of SS that can be isolated using s_R remote-controlled steps and s_M manual steps is locally equivalent to the dichotomic feeder associated with the pair (s_R, s_M).

The previous arguments can be used to show that the impact of a non-dichotomic feeder having the same number of SS can be calculated as the weighted average of dichotomous feeders by choosing for each branch the impact associated with the locally equivalent dichotomous feeder.

Figure 9 illustrates an example of a non-dichotomic feeder having 4 branches described by the dichotomic feeder associated with the pair (2,1) and the remaining 4 branches described by the dichotomic feeder associ-

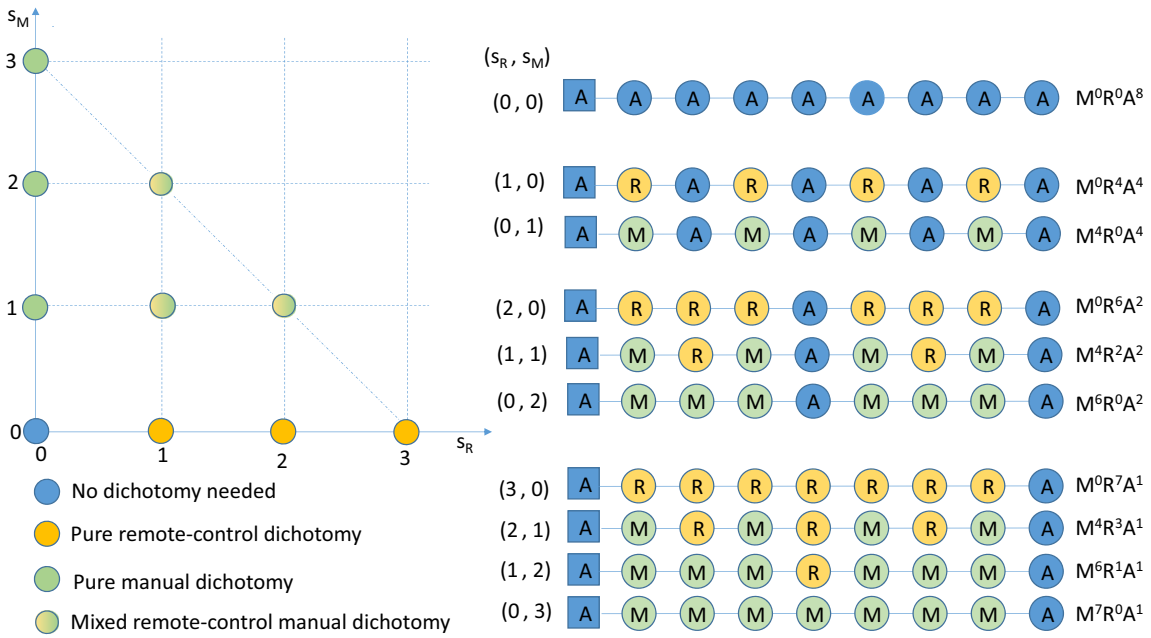

Fig. 8 Biunivocal relation between (s_R, s_M) pairs and dichotomic feeder

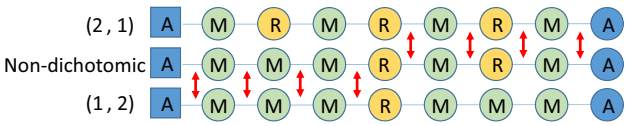

Fig. 9 Non-dichotomic feeder as weighted average of dichotomous feeders

ated with the pair (1,2) resulting in an impact equal to the mean of the two associated feeders impacts.

It is interesting to note that similar considerations can be made to study the effectiveness of technologies installed on a feeder. Indeed, it can be easily realized that the example shown in Fig. 9 can be also interpreted as not working remote-controlled SS of the (2,1) dichotomic feeder downgrading to a manual one. Alternatively, the failure of automated or remote-controlled SSs can be roughly modelled with a simple variable change: $N_A \rightarrow \eta_A N_A$; $N_R \rightarrow \eta_R N_R$ where η_A and η_R represent the efficiency of Automatic and Remote-control SSs, respectively. The efficiencies are defined as the percentage of automatic and remote-controlled SSs correctly operating during a selection with respect to the total number of N_A and N_R present on the feeder.

5 Application of the model

5.1 Application to a realistic scenario

In this section, an illustration of the model applied by areti spa to the feeders of the electrical grid of Rome—to make considerations about the planning of remote-controlled and automatic switches installation—is illustrated.

The proposed scenario presents a feeder having 8 SSs and a realistic set of parameters values obtained by means of suitable statistics on historical real data and summarized in Table 1.

The impact D_{Bil} given by (18) is calculated for each of the 10 possible dichotomous configurations existing for $N_{\text{TOT}} = 8$ (see Fig. 8) and listed in Table 2 as a function of the remote-controlled and manual steps needed to repower the feeder during the dichotomous procedure.

It is crucial to remark that the proposed model allows to focusing on 10 configurations only instead of using the $3^8 = 6.561$ possible configuration existing for an 8 CS long feeder.

Finally, the D_{Bil} impact normalized by its max value (i.e. when all the SS are manually maneuvered) and plotted as a function of the number of remote-controlled and manual steps needed to completely repower the feeder is shown in Fig. 10.

It should be noted that the plotted function presents an exact value only for integer values of s_R and s_M. Those points are highlighted in Fig. 10 with small ellipses on the surface and labelled with the value assumed by the function in that points.

Based on Fig. 10, it can be realized that the simple upgrading from manual to remote-controlled of the

Table 1 Realistic parameter set adopted for the calculations

N_{TOT}	t_{0R}	t_{0M}	t_R	t_M
8	1	45	4	10

Table 2 D_{Bil} of the 10 dichotomous configurations obtained for $\mathrm{N_{TOT}} = 8$: (a) absolute, (b) normalized by max, and (c) fundamental set-up

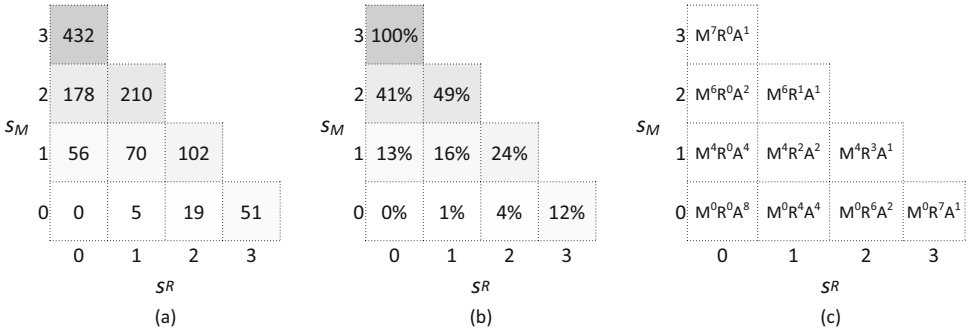

Fig. 10 Normalized D_{Bil} for an 8 SS long feeder

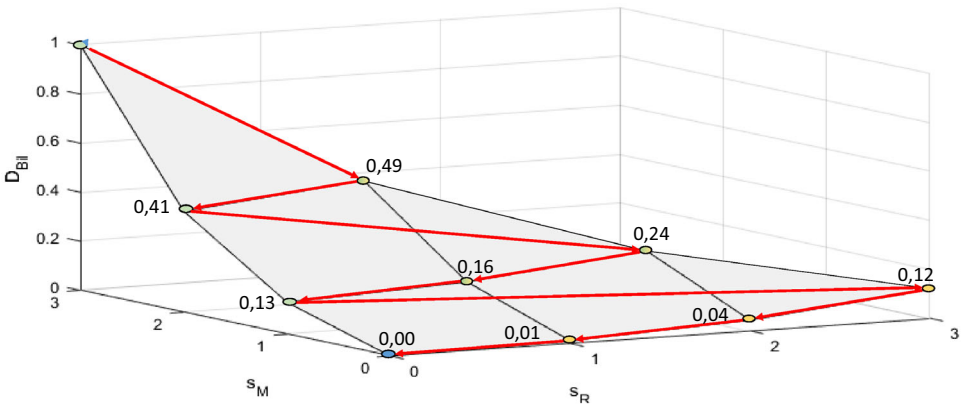

middle SS will result in a 51% reduction of the D_{Bil} impact with respect to the pure manual configuration, whereas the automation of the same SS will result in a benefit of 59%.

Moreover, the result of automating three of the seven manual SSs (benefit 87%) is approximately the same as remote-controlling all the seven manual SS (benefit 88%).

Finally, alternating remote-controlled and automated SSs along with the feeder results in only 99% of D_{Bil} impact reduction.

The previous statements are summarized in Table 3 where the benefit of upgrading a specified number of manual SSs in remote-controlled and automatic ones is listed.

To choose the best upgrade intervention, it is important to consider together with the benefit the cost of the intervention. This cost can be considered linear with the number of transformed manual SS taking care to consider that the cost of an automated SS is higher than that of a remote-controlled.

Finally, the objective function $F(s_R, s_m)$ to minimize can be obtained by adding the cost of the penalties associated with the impact of a given feeder with the cost of the technological intervention used to mitigate the impact as follows:

$$F(s_R, s_M) = \pi_D D_{\mathrm{Bil}}(s_R, s_M) + \pi_R N_R(s_R, s_M) + \pi_A N_A(s_R, s_M), \quad (23)$$

where π_D, π_R, and π_A represent the cost of a minute of impact, the cost of the transformation of a manual SS in a remote-controlled one, and the cost of the transformation of a manual SS in a remote-controlled one, respectively. The dependence on the variables (s_R, s_M) of the number N_R and N_A can be obtained using (4), (6), (8), and (9).

The solution of the stated problem is obtained by finding the pair (s_R, s_M) which minimizes (23) among the 10 dichotomic configurations listed in Fig. 8.

5.2 Real fault–impact versus model-forecast.

To validate the analytical approach proposed, a comparison among the fault impact predicted by the model and the real-impact registered during the faults that occurred upon the *a*reti grid during year 2020 and already certified to the authority is presented.

The comparison has been proposed for the U_{Uni} and D_{Uni} impact indicators of the unilateral automation only. This is because the bilateral automation is a new technology still being installed on *a*reti's grid and there are not yet historical fault-impact values available for the comparison. However, we guess that the prediction accuracy of the unilateral model is an underestimation of the accuracy reachable by the bilateral model. Indeed, unlike the bilateral automation model (which is exact under the given assumptions), the unilateral model estimates an average of all the possible impacts

Table 3 Benefit obtained from the upgrading of manual SSs in remote controlled and automated ones

Before upgrade			**After upgrade**			**MAN→REM**	**MAN→AUT**	**benefit %**
FS	(s_R, s_M)	$D_{\text{bil}}\%$	*FS*	(s_R, s_M)	$D_{\text{bil}}\%$			
$M^7R^0A^1$	(0,3)	100%	$M^6R^1A^1$	(1,2)	49%	1	0	51%
			$M^6R^0A^2$	(0,2)	41%	0	1	49%
			$M^4R^3A^1$	(2,1)	24%	3	0	66%
			$M^4R^0A^4$	(0,1)	13%	0	3	87%
			$M^0R^7A^1$	(3,0)	12%	7	0	88%
			$M^0R^4A^4$	(1,0)	1%	3	4	99%

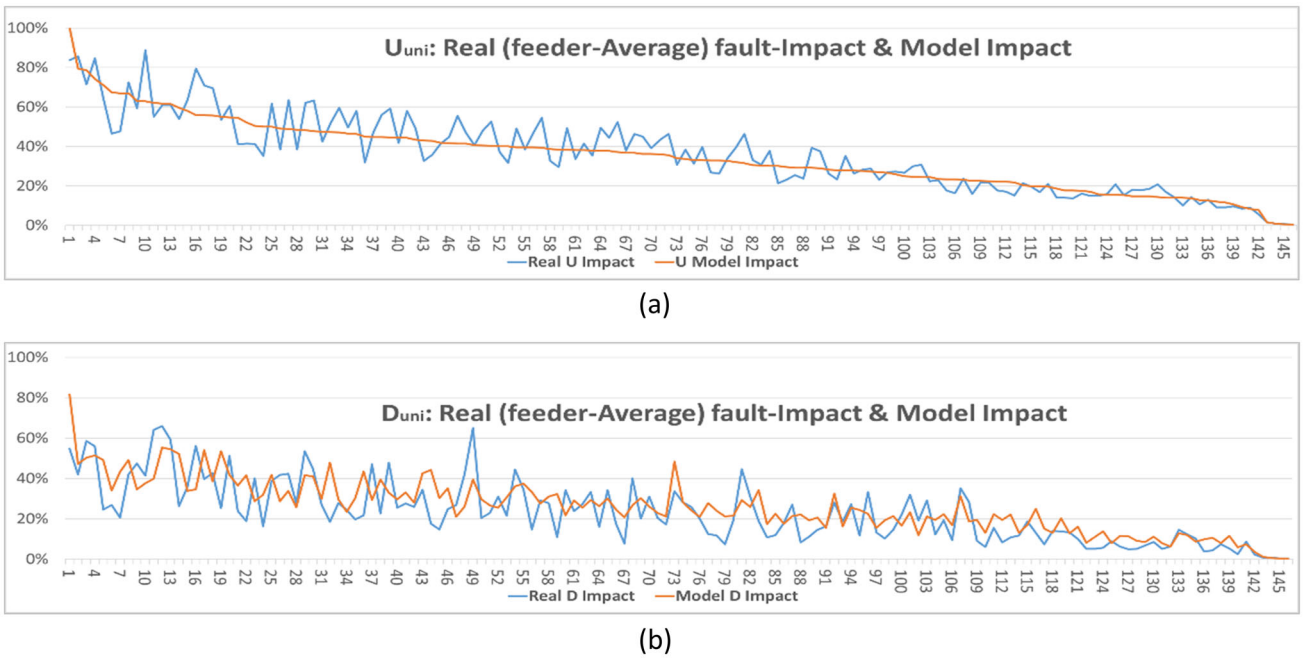

Fig. 11 Comparison between impact-model forecast and real data: **a** Uuni **b** Duni

scenarios, which depend on the position of each fault along the feeder.

To perform the comparison, a set of feeders has been selected according to the following requirements. Each selected feeder must present at least one fault that occurred during the year 2020 and the fault must not present events non-predictable by the model (e.g., contemporary multiple faults on a feeder).

According to the previous criteria, the comparison has been performed considering 145 real feeders belonging to *a*reti grid, which represents around 10% of the entire grid. It should be noted that in about 60% of the 145 feeders, there was more than one fault in 2020. In these cases, the average of the KPI of all the faults that occurred on the same feeder has been considered for comparison.

In Fig. 11 part (a) and (b) are shown the real fault impact average of the selected feeders (blue line) versus the model prediction (red line) for U_{Uni} and D_{Uni} KPIs, respectively. Feeders are ordered for descending U_{Uni} impact calculated by the model. The impact variables are normalized by the maximum impact calculated by the model.

The Pearson's correlation and the average error between the real data and the model prediction for U_{Uni} are 92% and 16,5%, respectively; whereas the Pearson's correlation and the average error between the real data and the model prediction for D_{Uni} are 74% and 35,5%, respectively

As expected, the prediction is more accurate for U_{Uni} than for D_{Uni} impact. Indeed, the duration impact strongly depends on uncertain variables related to the restoration sequence (e.g. traffic, human operator reaction time, etc.)

As already discussed, we believe that the analytical models are complementary to the more complex and precise numerical ones; indeed, the lack of accuracy is compensated by their simplicity and can help the DSO in its preliminary strategic planning.

6 Conclusion

The incoming challenge of the energy transition will strongly involve the Distribution System Operators

(DSO), especially when dealing with an urban context. In this context, optimal sizing and positioning of both automatic and remote-controlled switches and the knowledge of the effect of operational variables on the grid will become crucial, to assure the resilience of the entire urban system.

We strongly believe that the analytical approximated approach, which is proposed in this work to model the fault restoration process, gives a new useful supplemental tool for the DSO to better plan its interventions.

In this work, we have presented a new approach to the evaluation of the impact due to a fault in terms of: total time T needed to complete the service restoration, total number of disconnected users U, and sum of all user-interruption durations D (where U and D are at the base of the SAIFI and SAIDI indexes). These KPIs for the impact reduction have been derived for the bilateral automation case and they have been extended to the unilateral automation one. To obtain an analytical model, the idealistic hypothesis of the dichotomous structure of the feeder has been assumed. Nevertheless, the way to extend the obtained results from the dichotomous feeder structure into a more general uniform distribution of remote and automated SSs has been discussed. Moreover, the model has been extended to the case of non-ideal effectiveness of automated and remote-controlled switches. The model offers a way to analyze the variation of the KPI impact as a function of input variables, enabling to drive operational, maintenance, and grid development interventions. Finally, a simple application of how the model can be used for grid development planning and to drive investment planning is discussed.

Acknowledgements The authors would like to thank Anna Presciuttini for her contribution in revising the text and the contribution to the final editing.

Author contribution statement

S. Alessandroni ideated the novel analytical approach and derived the first rough model. F. Nicotra did the first implementation of the model, performed the bibliographic research, and formatted the text of the paper. M. Paschero gave the mathematical formalization of the problem and studied the application of the model in the dichotomous structure.

References

1. A. Tofani, G. D'Agostino, A. Di Pietro, S. Giovinazzi, L. La Porta, G. Parmendola, M. Pollino, V. Rosato: Modeling resilience in electrical distribution networks. Manag. Crit. Infrastruct. (2019), pp. 33–48
2. P. Pederson, D. Dudenhoeffer, S. Hartley, M. Permann, Critical infrastructure interdependency modeling: a survey of us and critical infrastructure interdependency modeling: a survey of U.S. and international research, technical report, Idaho National Laboratory (2006)
3. T. Petermann, H. Bradke, A. Lüllmann, M. Poetzsch, U. Riehm, in Office of Technology Assessment at the German Bundestag - Technology Assessment Studies Series. What happens during a blackout: consequences of a prolonged and wide-ranging power outage (2011)
4. A. Zidan, M. Khairalla, A.M. Abdrabou, T. Khalifa, K. Shaban, A. Abdrabou, R. El Shatshat, A.M. Gaouda, Fault detection, isolation, and service restoration in distribution systems: state of the art and future trends. IEEE Trans. Smart Grid **8**(5), 2170–2185 (2017)
5. L. Mili, M. Panteli, J. Kavicky, K. Thomas, R. Desalvo, J. Liu, H. Chao, IEEE technical report PES-TR65 (2018)
6. Council of European Energy Regulators, 6th CEER benchmarking report on the quality of electricity and gas supply (2016)
7. D. Fioriti, D. Poli, Fault localization to improve power system quality in distribution networks: a greedy approach to optimize the switching sequence of remotely-controlled devices. IEEE Madrid PowerTech (2021)
8. A. Ajith, D. Swagatam, *Computational Intelligence in Power Engineering* (Springer, Berlin, 2010)
9. I.-H. Lim, B.-N. Ha, An optimal composition and placement of automatic switches in DAS. IEEE Trans. Power Deliv. **28**(3), 1474–1482 (2013)
10. Ž. Popović, S. Knezević, B. Brbaklić, Optimal reliability improvement strategy in radial distribution networks with island operation of distributed generation. IET Gener. Transm. Distrib. **12**(1), 78–87 (2018)
11. L. Silva de Assis, J. Federico Vizcaıó González, F. Luiz Usberti, C. Lyra, C. Cavellucci, F.J. Von Zuben, Switch allocation problems in power distribution systems. IEEE Trans. Power Syst. **30**, 246–253 (2015)
12. L.G. Weszda Silva, R.A. Fernandes Pereiraa, J. Rivier Abbad, J.R. Sanches Mantovani, Optimised placement of control and protective devices in electric distribution systems through reactive Tabu search algorithm. Electr. Power Syst. Res. **78**, 372–381 (2008)
13. J.-M. Sohn, S.-R. Nam, J.-K. Park, Value-based radial distribution system reliability optimization. IEEE Trans. Power Syst. **21**, 941–947 (2006)
14. L. Wang, C. Singh, Reliability-constrained optimum placement of reclosers and distributed generators in distribution networks using an ant colony system algorithm. IEEE Trans. Syst. Man Cybern. Part C (Appl. Rev.) **38**, 757–764 (2008)
15. A. Vieira Pombo, J. Murta-Pina, V. Fernão Pires, A multiobjective placement of switching devices in distribution networks incorporating distributed. Electr. Power Syst. Res. **130**, 34–45 (2016)
16. D. Popović, S.D. Knezevic, Z.N. Popovic, Risk-based allocation of automation devices in distribution networks with performance-based regulation of continuity of supply. IEEE Trans. Power Syst. **34**, 171–181 (2019)
17. J.C. López, J.F. Franco, M.J. Rider, Optimization-based switch allocation to improve energy losses and service restoration in radial electrical distribution systems. IET Gener. Transm. Distrib. **10**(11), 2792–2801 (2016)

18. J. Nahman, D. Perić, Distribution system performance evaluation accounting for data uncertainty. IEEE Trans. Power Del. **18**, 694–700 (2003)
19. O.K. Siirto, A. Safdarian, M. Lehtonen, M. Fotuhi-Firuzabad, Optimal distribution network automation considering earth fault events. IEEE Trans. Smart Grid **19**(2), 1010–1018 (2015)
20. R.P.Y. Mehairjan, D. Djairam, Q. Zhuang, J.J. Smit, A.M. van Voorden, Statistical life data analysis for electricity distribution cable assets—an asset management approach. In: IET and IAM Asset Management Conference (2011)
21. H. Wang, D. Lin, J. Qiu, L. Ao, Z. Du, B. He, Research on multiobjective group decision-making in condition-based maintenance for transmission and transformation equipment based on D-S evidence theory. IEEE Trans. Smart Grid **6**(2), 1035–1045 (2015)
22. M. Cheng, Y. Zeng, R. Niu, Y. Chen, Study on the model of advanced asset management in smart grid. In: 4th International Conference on Electric Utility Deregulation and Restructuring and Power Technologies (DRPT) (2011)
23. H. Zaki, R.A. Swief, T.S. Abdel-Salam, M. Mostafa, A new distribution system performance approach to the switch allocation problem under smart grid framework. In: E3S Web of Conferences (2018)
24. S. Lei, J. Wang, Y. Hou, Remote-controlled switch allocation enabling prompt restoration of distribution systems. IEEE Trans. Power Syst. **33**, 3129–3142 (2018)
25. A. Zeinalzadeh, A. Estebsari, A. Bahmanyar, Multi-objective optimal placement of recloser and sectionalizer in electricity distribution feeders. In: IEEE International Conference on Environment and Electrical Engineering and 2019 IEEE Industrial and Commercial Power Systems Europe (EEEIC / I&CPS Europe), pp. 1–4 (2019)
26. Y. Xu, C.-C. Liu, K.P. Schneider, D.T. Ton, Placement of remote-controlled switches to enhance distribution system restoration capability. IEEE Trans. Power Syst. **31**(2), 1139–1150 (2016)
27. C.-H. Lin, H.-J. Chuang, C.-S. Li, M.-Y. Huang, C.-W. Huang, Optimal placement of line switches for distribution automation systems using immune algorithm. IEEE Trans. Power Syst. **21**, 1209–1217 (2006)
28. A. Tofani, G. D'Agostino, A. Di Pietro, S. Giovinazzi, M. Pollino, V. Rosato, S. Alessandroni, Operational resilience metrics for complex inter-dependent. Appl. Sci. **11**(13), 1–28 (2021)